applied sciences

MDPI

Article

Chalcogenide–Tellurite Composite Photonic Crystal Fiber: Extreme Non-Linearity Meets Large Birefringence

Amir Ahmadian [1] and Yashar Esfahani Monfared [2,*]

[1] Department of Electrical Engineering, Science and Research Branch, Azad University, Tehran 1477893855, Iran; amir.ahmadian@ieee.org
[2] Department of Physics and Atmospheric Science, Dalhousie Univeristy, Halifax, NS B3H 4R2, Canada
* Correspondence: y.monfared@dal.ca

Received: 25 September 2019; Accepted: 15 October 2019; Published: 19 October 2019

Abstract: In this paper, we propose a novel design of a photonic crystal fiber (PCF) with tellurite-cladding, three rings of air-holes and elliptical concentration of As_2S_3 in the fiber core. The combined effect of tight mode confinement (an effective mode area of nearly 0.6 μm^2), large non-linear refractive index of As_2S_3 and significant variation between the effective modal index values of the two orthogonal states of the fundamental guided mode leads to extreme non-linear coefficient and birefringence values, all achieved at the zero dispersion wavelength (ZDW) of 1550 nm. The corresponding birefringence and non-linear coefficient (7×10^{-3} and 28 W^{-1} m^{-1}, respectively) are more than three orders of magnitude larger than that of the regular silica-based highly non-linear PCFs. In addition, we numerically demonstrate that by modifying the core and air-hole dimensions one can easily control the dispersion curve and tune the ZDW of the proposed fiber to any excitation wavelength ranging from near-infrared to short-wave-infrared, including optical telecommunication windows close to 1550 nm. The superior characteristics of the proposed elliptical-core composite PCF including extreme non-linearity, nearly-zero confinement loss (2.47×10^{-12} dB/cm), the ability to maintain polarization of light, and tunable ZDW can open the door to new possibilities in non-linear optics, optical telecommunications, optical signal processing, and sensing devices.

Keywords: photonic crystal fiber; chalcogenide glass; nonlinear optics

1. Introduction

The design and development of compact non-linear devices based on highly non-linear photonic crystal fibers (HNL-PCFs) have attracted much attention in both academia and industry over the last decade [1]. HNL-PCFs can be used as a non-linear medium to realize all-optical wavelength conversion [2], supercontinuum generation [3], pulse compression [4], and parametric amplification [5]. According to Miller's rule [6], third-order optical non-linearity of the glass strongly depends on the linear refractive index. As silica glass does not exhibit large linear and non-linear refractive indices (nearly 1.45 and 2.9×10^{-20} m^2/W, respectively, at optical communication wavelengths near 1550 nm), a long fiber length and/or huge power levels are usually required to utilize non-linear effects [7]. These requirements render the silica-based HNL-PCFs limited in most of the non-linear applications, especially in terms of costs and practicality.

To realize non-linear processes with low powers and in short interaction lengths, non-silica photonic crystal fibers (PCFs) made of high-index glasses such as tellurite [8], bismuth-oxide [9], and chalcogenide glasses [10] as well as PCFs filled with high-index liquids such as carbon-disulfide [11,12] are designed, studied and fabricated. Among different materials, chalcogenide glasses with a large refractive index of around 3, ultra-high non-linear refractive index of 3×10^{-18} m^2/W, and a high transmission window from 0.6 to 15 μm, open up new possibilities to design and develop compact non-linear devices [13]. However, this great potential of chalcogenide fibers is limited in real-world applications due to the relatively large material dispersion of chalcogenide glasses in visible and near-infrared regions. Chalcogenide nano-fibers or nano-wires [13] can solve the problem by shifting the zero dispersion wavelength (ZDW) of chalcogenide from mid-IR to near optical telecommunication bands [14]. Unfortunately, nano-wires are fragile and the degradation in their surface is a crucial challenge that has not been resolved yet. For example, in the environment of a conventional optics laboratory the air cladding nano-wires fail completely within a few weeks [13,14]. PCFs can solve the dispersion problem of chalcogenide glasses by shifting the ZDW from mid-IR to a near-IR band using an appropriate material selection and array of air-holes in the cladding. The composite PCF with As_2S_3 core and tellurite cladding, with a ZDW in near-IR and stable optical properties has been fabricated successfully before [13,14]. The use of tellurite glass in the cladding region can protect the core glass from the degradation over time and also can minimizes toxicity concerns about As_2S_3.

Furthermore, highly birefringent PCFs have been developed during the last few years for applications in temperature, pressure and refractive-index sensing [15,16], single-polarization-single-mode communications [17], polarization-sensitive optical modulators [18], and polarization-maintaining linear and non-linear devices [19]. Birefringence appears due to the asymmetry in fiber structure, which causes a huge difference between the effective refractive index of x-axis and y-axis polarized modes [19]. If this difference is greater than 1×10^{-4}, the modes are quite separated and the fiber is considered to be highly birefringent.

In this paper, we design extremely non-linear composite tellurite-chalcogenide PCFs with circular holes and study the optical properties of PCF (nonlinear coefficient, dispersion, loss, and birefringence) in detail. To achieve polarization maintaining, we introduce an asymmetry in the PCF structure by using an elliptical core to induce a large birefringence in the fiber. We then compare all of the optical characteristics of the proposed elliptical-core PCF with a regular circular-core PCF to highlight the differences between two designs. The proposed elliptical-core composite PCF has a small effective area, extremely large non-linear coefficient, controllable dispersion, and a huge birefringence of 7×10^{-3} near optical communication windows. The combined effect of huge non-linearity, tunable dispersion and large birefringence can lead to interesting applications of our proposed PCF in ultra-compact non-linear devices, in future optical signal processing devices, sensors, and optical telecommunication networks.

2. Fiber Design

Our proposed composite PCF has a tellurite glass cladding with three rings of air holes in a hexagonal lattice, surrounding an As_2S_3-core in the center of the fiber. We use Sellmeier's equation [7] to find the amount of linear refractive index of materials in different excitation wavelengths,

$$n^2(\lambda) = 1 + \sum_{j=1}^{k} \frac{A_j \lambda^2}{\lambda^2 - B_j^2} \tag{1}$$

where A_j and B_j are Sellmeier's coefficients, λ is the excitation wavelength in micrometers and $n(\lambda)$ is the wavelength-dependent linear refractive index of material [7]. The Sellmeier's coefficients for As_2S_3 are A_1 = 1.8983678, A_2 = 1.9222979, A_3 = 0.8765134, A_4 = 0.1188704, A_5 = 0.9569903, and B_1 = 0.15, B_2 = 0.25, B_3 = 0.35, B_4 = 0.45 and B_5 = 27.3861 (μm^{-2}) [13]. Therefore, one can find the refractive index of As_2S_3 as a function of wavelength using the following equation,

$$n^2 = 1 + \frac{1.8983678\lambda^2}{\lambda^2 - 0.0225} + \frac{1.9222979\lambda^2}{\lambda^2 - 0.0625} + \frac{0.8765134\lambda^2}{\lambda^2 - 0.1225} + \frac{0.1188704\lambda^2}{\lambda^2 - 0.2025} + \frac{0.9569903\lambda^2}{\lambda^2 - 750}. \tag{2}$$

The composition of the tellurite glass is considered to be $76.5TeO_2$-$6Bi_2O_3$-$11.5Li_2O$-$6ZnO$ (mol%), which is the same as that of the tellurite glass in [13,14]. The Sellmeier's coefficients for this tellurite glass are A_1 = 1.67189, A_2 = 1.34862, A_3 = 0.62186, and B_1 = 0.0216, B_2 = 0.23971 and B_3 = 6.8356 (μm^{-2}) [13]. Similar to As_2S_3, one can find the refractive index of tellurite as a function of wavelength using the following equation

$$n^2 = 1 + \frac{1.67189\lambda^2}{\lambda^2 - 0.00046656} + \frac{1.34862\lambda^2}{\lambda^2 - 0.0574608841} + \frac{0.62186\lambda^2}{\lambda^2 - 46.72542736}. \quad (3)$$

The material dispersion of As_2S_3 and tellurite glass can be easily calculated using the dispersion formula, $D_{material} = -\frac{\lambda}{c}\frac{d^2 n_{material}}{d\lambda^2}$ [20]. The linear refractive index and material dispersion of As_2S_3 and tellurite from visible (500 nm) to mid-infrared (3000 nm) are shown in Figure 1a,b as a function of wavelength.

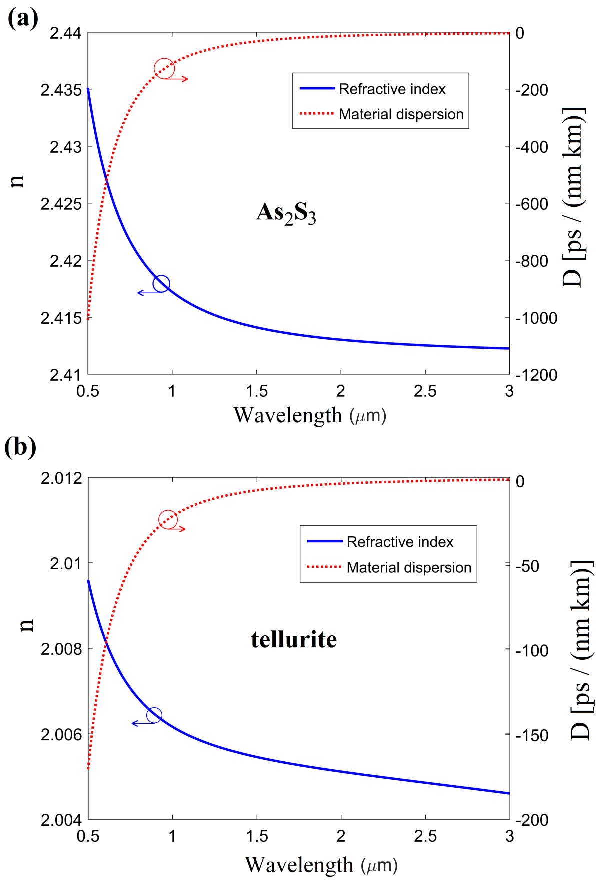

Figure 1. Linear refractive index and material dispersion of (**a**) As_2S_3 and (**b**) tellurite glass as a function of wavelength. The solid blue curve and left vertical axis represent refractive index values, and dotted red curve and right vertical axis represent material dispersion.

The design parameters of the circular-core composite PCF (C-PCF) are the hole diameter d, hole pitch Λ, and core diameter d_c. In the case of elliptical core composite PCF (E-PCF), instead of core diameter we have two new parameters: width a, and height b of the ellipse. The cross sections of the proposed PCFs are shown in Figure 2.

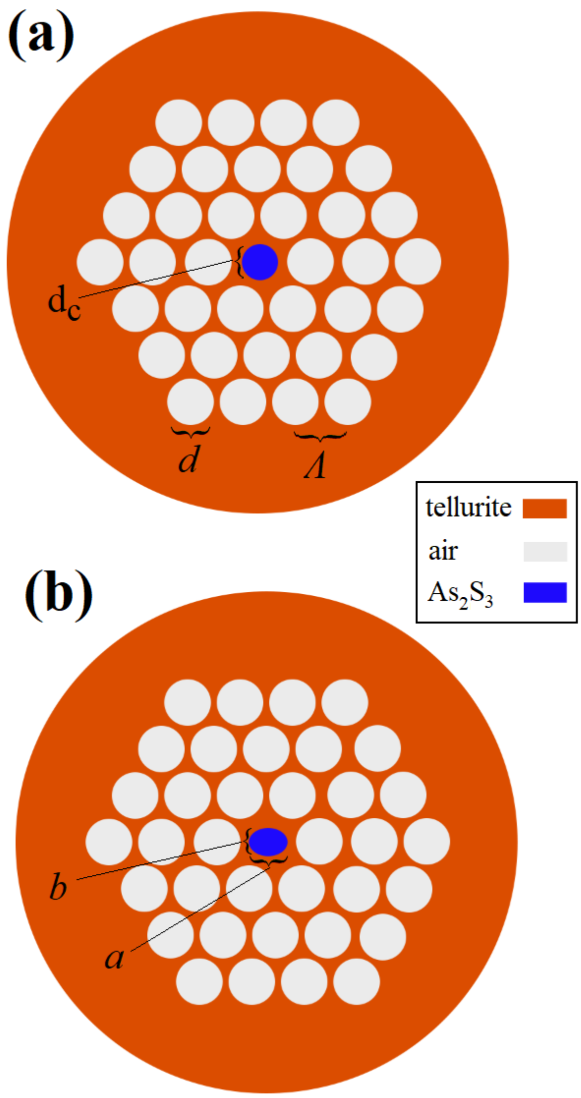

Figure 2. The cross-section of the proposed composite photonic crystal fiber (PCF) with tellurite in cladding, three rings of air-holes and As_2S_3 in (**a**) a circular core and (**b**) an elliptical core.

3. Results and Discussion

Using a numerical finite difference time domain (FDTD) method [21,22], we calculate the effective modal index of fundamental guided mode (n_{eff}) and study the effective mode area, non-linear coefficient, birefringence, confinement loss, and dispersion properties of our proposed PCFs. In the numerical analysis, we consider the case of mode confinement in the PCF core through total internal reflections (TIR). The calculated n_{eff} is strongly dependent on the design parameters, especially air hole arrangement in the cladding of the PCF. Note that the design parameters of PCFs in this paper are optimized for optical telecommunications windows near 1550 nm (1100 nm to 1900 nm).

3.1. Dispersion

Fiber dispersion is a key player in determining the efficiency of non-linear processes in optical fibers as it usually determines the phase-matching conditions [2,7]. The dispersion is calculated as the sum of wave-guide and material dispersions ($D = D_{material} + D_{waveguide}$) [20]. In our simulations, the material dispersion of As_2S_3 and tellurite glass (as illustrated in Figure 1) has been taken into account. Due to large material dispersion of As_2S_3 in near-infrared and short-wave-infrared, we should compensate material dispersion using the wave-guide dispersion of the PCF. The wave-guide dispersion in PCFs can be easily controlled by modifying the air hole dimensions, numbers and center-to-center pitch. The dispersion characteristics of a fiber is usually calculated in terms of the dispersion parameter D, defined as [2,7]

$$D = -\frac{\lambda}{c}\frac{d^2 n_{eff}}{d\lambda^2} \tag{4}$$

where n_{eff} is the effective modal index of guided mode in the PCF core. The dispersion curve of C-PCF and E-PCF with different core dimensions and d = 0.692, Λ = 0.867, a = 1 µm as a function of wavelength is illustrated in Figure 3.

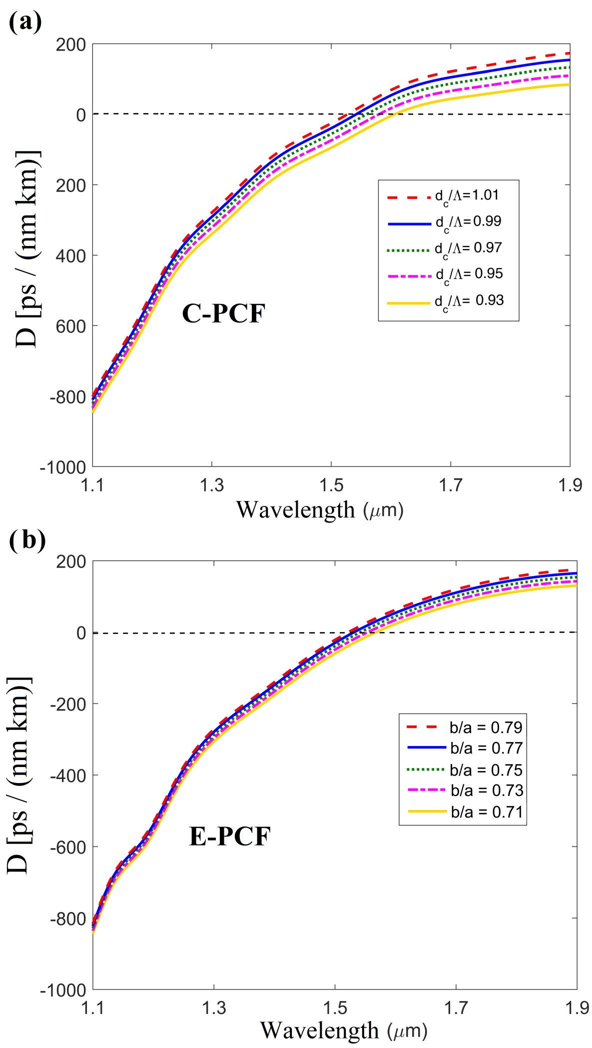

Figure 3. Dispersion of (**a**) circular-core fiber (C-PCF) and (**b**) elliptical-core fiber (E-PCF) with different core dimensions as a function excitation wavelength. The C-PCF parameters are: d = 0.692, Λ = 0.867, and E-PCF parameter is a = 1 µm.

As seen in Figure 3, by changing the core dimension ZDW can be tuned to different excitation wavelengths near 1550 nm. In particular, by increasing d_c/Λ from 0.93 to 1.01 in C-PCF (Figure 3a), ZDW shifts from 1.61 µm to 1.53 µm. This tunability of ZDW exists in a wide range of wavelengths in our proposed composite PCF (ZDW can be tuned from 1100 nm to 1900 nm). The same trend exist in E-PCFs. For example, as seen in Figure 3b, by increasing b/a from 0.71 to 0.79, ZDW shifts from 1.57 µm to 1.52 µm. In Figure 4, we study the effect of air-hole dimensions on the dispersion characteristics of C-PCFs and E-PCFs.

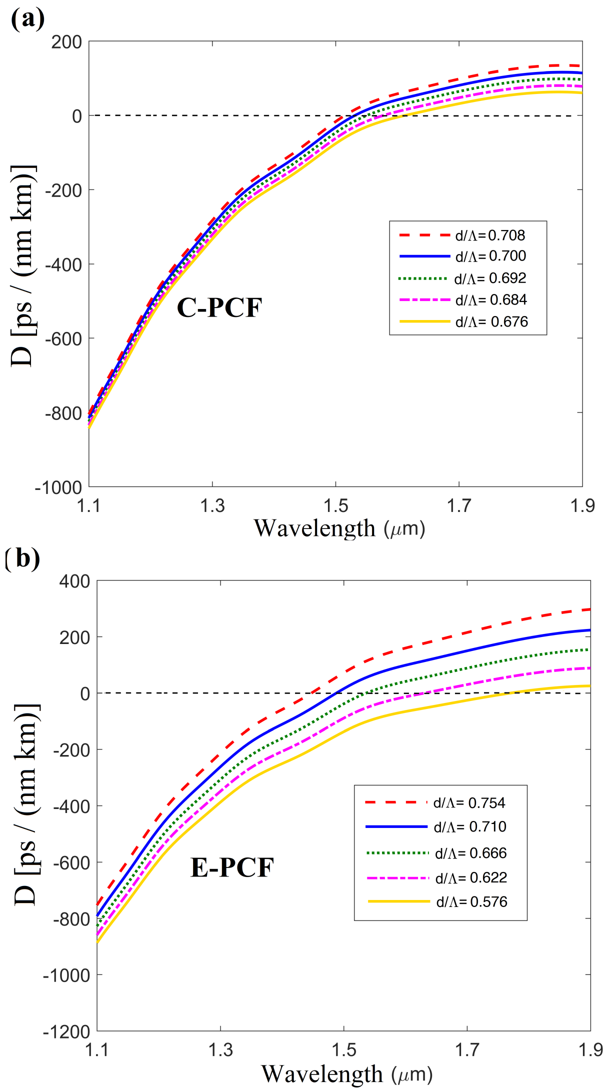

Figure 4. Dispersion of (**a**) C-PCF and (**b**) E-PCF with different air-hole dimensions as a function excitation wavelength. The C-PCF parameters are: $d_c/\Lambda = 0.876$, $\Lambda = 0.867$, and E-PCF parameters are $b/a = 0.79$ and $a = 1$ µm.

ZDW is sensitive to hole-dimensions in the cladding of the PCF. As seen in Figure 4a, by increasing d/Λ from 0.676 to 0.692, the ZDW shifts from 1.61 µm to 1.51 µm. In E-PCFs this shift in ZDW is even more sensitive to hole dimensions. As seen in Figure 4b, increasing d/Λ from 0.576 to 0.754 can result in a shift in ZDW from 1.77 µm to 1.45 µm. We confer that ZDW in both E-PCFs and C-PCFs is totally controllable by modifying the hole and/or core dimensions. Additionally, for a E-PCF with $d/\Lambda = 0.692$, $\Lambda = 0.867$µm, $b/a = 0.75$ and $a = 1$ µm, the ZDW is at 1550 nm, which is the wavelength of interest in optical communications.

3.2. Confinement Loss

The loss in optical fibers, especially PCFs, can have different origins including intrinsic material absorption, structural imperfection, micro or macro bending losses or confinement loss [22,23]. The periodic cladding of PCFs causes a decrease in optical confinement, which is called the confinement loss (CL) [23,24]. The imaginary part of the effective modal refractive index of guided modes $Im(n_{eff})$ is related to CL through the following equation [23,24]

$$CL = \frac{40\pi Im(n_{eff})10^6}{\lambda Ln(10)}. \tag{5}$$

CL is determined by the geometry of the PCF, especially the number (and size) of air holes in the cladding [23]. We investigate the relationship between CL and the number of air-hole rings in the cladding of the PCF with a 1550 nm excitation. As seen in Figure 5, by increasing the number of air-hole rings from one to three, the CL decreases significantly in both E-PCF and C-PCF. In E-PCF, the CL decreases from 0.002 dB/cm to 2.47 $\times$ 10^{-12} dB/cm, which is equal to nearly nine orders of magnitude. We saw the same pattern at different excitation wavelengths and with different air-hole dimensions. However, after $N = 3$, further increases in the number of air-hole rings does not have a significant impact on the magnitude of CL. Therefore, we confer that three rings of air-holes in a hexagonal-lattice PCF (in our excitation wavelengths) is the optimal number of air-holes, as more air-hole rings would increase the fabrication difficulty and fabrication-induced imperfections without any significant gain. However, the total loss in our proposed PCF is strongly dependent on absorption, fabrication-induced losses, and scattering losses of As_2S_3 and tellurite glass, which is estimated to be less than 1 dB/m at 1550 nm [13,14]. Excess losses during the fabrication are related to the interface between the capillaries, which is discussed in detail in [25].

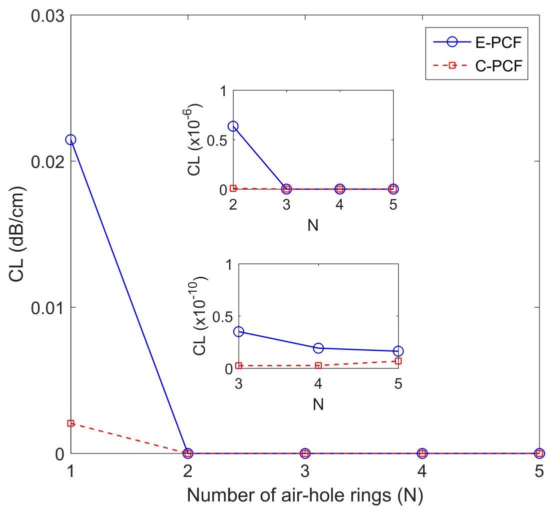

Figure 5. Confinement loss (CL) of PCF with circular-core and elliptical-core as a function of the number of air-hole rings at 1550 nm. The C-PCF parameters are: d/Λ = 0.692, d_c/Λ = 0.876 and Λ = 0.867 µm, and E-PCF parameters are b/a = 0.75 and a = 1 µm. The insets show the trend of CL for $N > 2$ (top inset) and $N > 3$ (bottom inset).

3.3. Birefringence

In a highly birefringent PCF, there is a significant variation between propagation constants of the two orthogonally polarized modes [23]. Due to this difference, the coupling between x-polarized and y-polarized modes decreases significantly [23]. Under these circumstances, the state of polarization of incident light can be maintained along the PCF provided that the light is coupled to only one of the polarized modes [26,27]. The birefringence is defined as [26,27]

$$B = n_x - n_y \tag{6}$$

where n_x and n_y are the effective modal index values of the two orthogonal states of the fundamental guided mode in the PCF core. To investigate polarization dependent and birefringence characteristics of our proposed PCF, we first investigate the fundamental guided mode in the fiber core with circular and elliptical core structures. The fundamental guided modes at 1550 nm for a C-PCF with $d/\Lambda = 0.692$, $d_c/\Lambda = 0.876$ and $\Lambda = 0.867$ µm , and E-PCF with $b/a = 0.75$ and $a = 1$ µm are illustrated in Figure 6a,b, respectively.

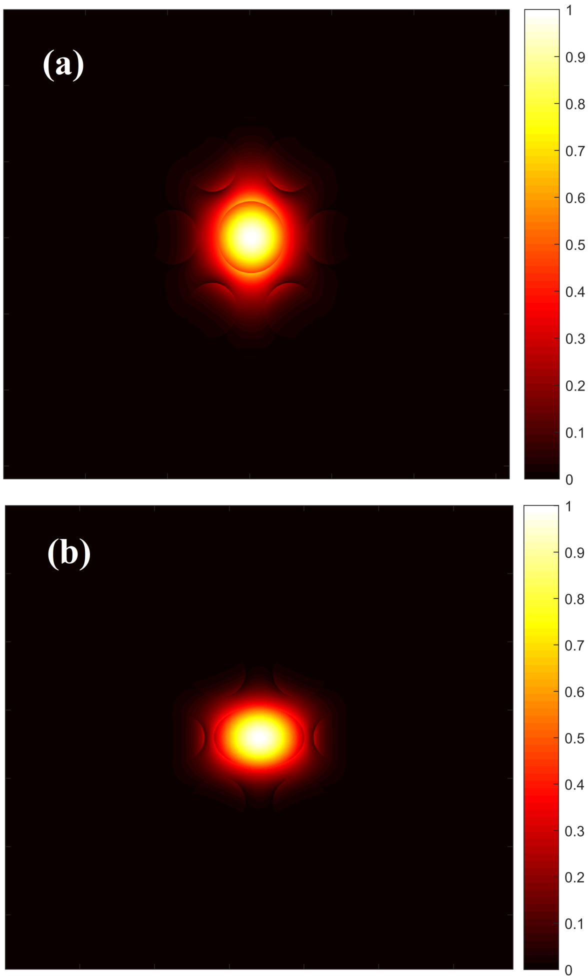

Figure 6. Intensity distribution of fundamental guided mode in (**a**) C-PCF with $d/\Lambda = 0.692$, $d_c/\Lambda = 0.876$ and $\Lambda = 0.867$ µm, and (**b**) E-PCF with $b/a = 0.75$ and $a = 1$ µm with a 1550 nm excitation.

According to Figure 6, we expect to see a nearly equal coupling for x-polarized and y-polarized light in the case of circular-core. We investigate the effective modal index for x-polarized and y-polarized light and the values of birefringence for circular-core and elliptical-core PCFs in different excitation wavelengths ranging from 1.1 to 1.9 µm in Figure 7.

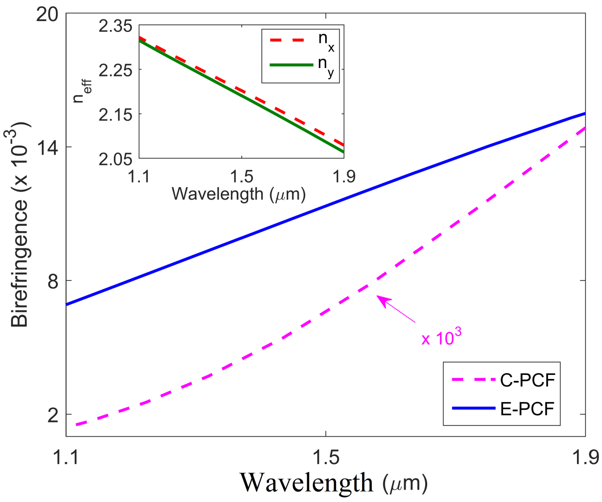

Figure 7. Birefringence of C-PCF with circular-core and elliptical-core as a function of wavelength. The C-PCF parameters are: $d/\Lambda = 0.692$, $d_c/\Lambda = 0.876$, $\Lambda = 0.867$ µm, and E-PCF parameters are $b/a = 0.75$ and $a = 1$ µm. The inset show effective modal indices of fundamental guided mode of E-PCF for x-polarized and y-polarized light. Note that the birefringence of circular-core PCF is enhanced by three orders of magnitude to facilitate visualization.

As seen in Figure 7, the elliptical-core PCF clearly shows a superior birefringence (more than three orders of magnitude larger than that of circular-core) due to structural asymmetry induced by the ellipse. The magnitude of birefringence in E-PCF at 1550 nm is nearly 7×10^{-3}, which is much larger than threshold value for high-birefringence fibers (1×10^{-4}). This fact clearly shows the ability of the proposed PCF to maintain the polarization of light, which can lead to different applications ranging from sensors to optical signal processing and optical communications.

3.4. Effective Mode Area and Non-Linear Coefficient

In most non-linear optical processes, one of the key factors to determine the efficiency of the non-linear medium is the non-linear coefficient [2]. The non-linear coefficient γ in an optical fiber is defined as [2,7]

$$\gamma = \frac{2\pi n_2}{\lambda A_{eff}}, \tag{7}$$

where n_2 is a non-linear refractive index of the core material and A_{eff} is an effective mode area of the fundamental guided mode in the fiber core, defined as [2,7]

$$A_{eff} = \frac{\int\int(|E|^2 dA)^2}{\int\int(|E|^4 dA)}. \tag{8}$$

The effective area and non-linear coefficient of a C-PCF and E-PCF with $d = 0.692$, $\Lambda = 0.867$, $a = 1$ µm is shown in Figure 8.

As seen in Figure 8, the effective mode area increases gradually with an increase in excitation wavelength and consequently, the non-linear coefficient decreases with an increase in excitation wavelength. It is evident that extremely large non-linear coefficients of 15 to 45 W^{-1} m^{-1} can be achieved in our proposed composite PCFs with both circular and elliptical cores. These values are more than three orders of magnitude larger than that of a regular silica-based HNL-PCF and more than one order of magnitude larger than that of a liquid-filled HNL-PCF [7]. The combined effect of tight mode confinement in an As_2S_3 core and large n_2 of chalcogenide glasses, particularly 3×10^{-18} m^{-1} W^{-1} for As_2S_3 [13], leads to the large non-linear coefficients in our proposed PCFs. The proposed fiber with such a huge nonlinearity, tunable dispersion, and large birefringence can have applications in different nonlinear processes where phase matching is important (for example wavelength conversion via four-wave mixing), and applications where the polarization maintaining is important (like sensing via a Sagnac interferometer).

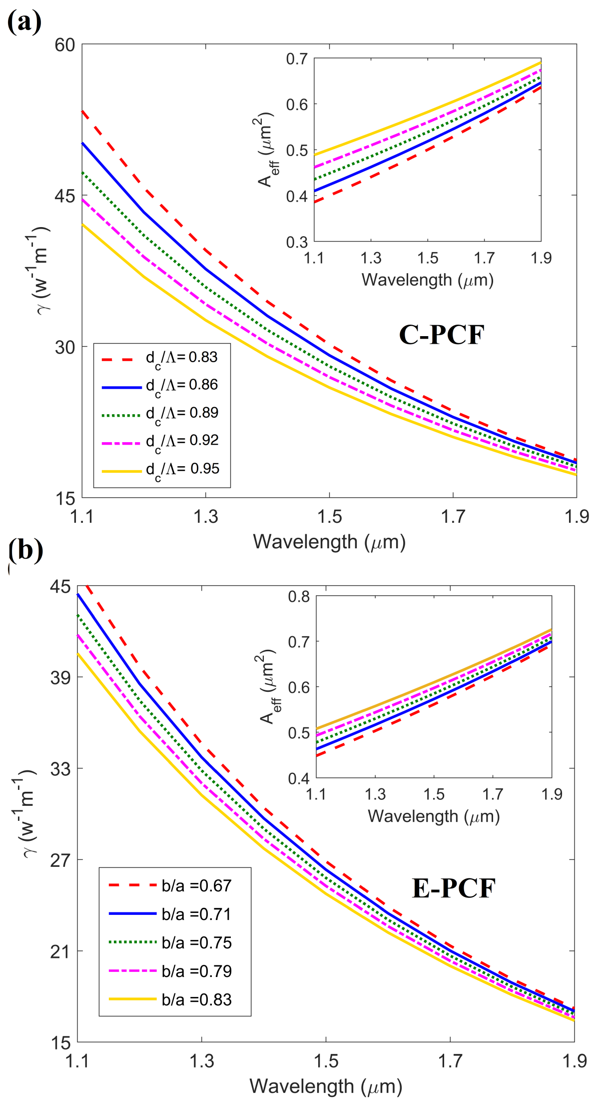

Figure 8. Non-linear coefficient (main plots) and effective mode area (inset plots) of PCFs with (**a**) circular-core, and (**b**) elliptical-core, with different core dimensions as a function of excitation wavelengths. The C-PCF and E-PCF parameters are: d = 0.692, Λ = 0.867, a = 1 µm.

4. Conclusions

We designed a novel composite chalcogenide-core tellurite-cladding photonic crystal fiber (PCF) with high non-linearity, high birefringence, and a tunable zero dispersion wavelength using a numerical approach. By utilizing an elliptical-core, three rings of air-holes, and realistic hole dimensions, we obtained an ultra small effective mode area of nearly 0.6 µm^2, a huge non-linear coefficient of 28 W^{-1} m^{-1}, a large birefringence of 7 $\times 10^{-3}$, nearly-zero confinement loss of 2.47 $\times$ 10^{-12} dB/cm, and a zero dispersion at 1550 nm. We compared all of the optical characteristics of the proposed elliptical-core PCF with a regular circular-core PCF to highlight the differences between the two designs. We further showed that by modifying the core and air-hole dimensions one can easily control the dispersion curve and tune the zero dispersion wavelength of the proposed fiber to any excitation wavelength ranging from near-infrared to short-wave-infrared, including optical telecommunication windows close to 1550 nm. The proposed PCF with large non-linearity, polarization-maintaining capabilities, and the possibility of tuning zero dispersion wavelengths, could have important applications in non-linear optics, optical telecommunications, optical signal processing and even sensing devices.

Author Contributions: A.A. (investigation, data curation, software, methodology, formal analysis); Y.E.M. (visualization, formal analysis, validation, writing–original draft, writing–review and editing, project administration

Funding: This research received no external funding. Y.E.M. acknowledge the support of the Dalhousie University and Killam trusts.

Conflicts of Interest: The authors declare no conflict of interest.

References

1. Russell, P.S.J. Nonlinear Optics in Photonic Crystal Fiber: Recent Developments. In Proceedings of the Lasers Congress 2016 (ASSL, LSC, LAC) OSA Technical Digest, Online, Optical Society of America, Boston, MA, USA, 30 October–3 November 2016.
2. Monfared, Y.E.; Mojtahedinia, A.; Javan, A.R.M.; Monajati Kashani, A.R. Highly nonlinear enhanced-core photonic crystal fiber with low dispersion for wavelength conversion based on four-wave mixing. *Front. Optoelectron.* **2013**, *6*, 297–302. [CrossRef]
3. Balani, H.; Singh, G.; Tiwari, M.; Janyani, V.; Kumar Ghunawat, A. Supercontinuum generation at 1.55 µm in As_2S_3 core photonic crystal fiber. *Appl. Opt.* **2018**, *57*, 3524–3533. [CrossRef] [PubMed]
4. Mosley, P.J.; Huang, W.C.; Welch, M.G.; Mangan, B.J.; Wadsworth, W.J.; Knight, J.C. Ultrashort pulse compression and delivery in a hollow-core photonic crystal fiber at 540 nm wavelength. *Opt. Lett.* **2010**, *35*, 3589–3591. [CrossRef] [PubMed]
5. Singh, S.P.; Varshney, S.K. Tunable optical parametric amplification characteristics of liquid-filled chalcogenide photonic crystal fibers. *Opt. Lett.* **2013**, *38*, 3846–3849. [CrossRef]
6. Sugimoto, N.; Kanbara, H.; Fujiwara, S.; Tanaka, K.; Shimizugawa, Y.; Hirao, K. Third-order optical nonlinearities and their ultrafast response in Bi_2O_3–B_2O_3–SiO_2 glasses. *J. Opt. Soc. Am. B* **1999**, *16*, 1904–1908. [CrossRef]
7. Monfared, Y.E.; Ponomarenko, S.A. Extremely nonlinear carbon-disulfide-filled photonic crystal fiber with controllable dispersion. *Opt. Mater.* **2019**, *88*, 406–411. [CrossRef]
8. Xu, F.; Yuan, J.; Mei, C.; Li, F.; Kang, Z.; Yan, B.; Zhou, X.; Wu, Q.; Wang, K.; Sang, X.; et al. Mid-Infrared Self-Similar Pulse Compression in a Tapered Tellurite Photonic Crystal Fiber and Its Application in Supercontinuum Generation. *J. Lightw. Technol.* **2018**, *36*, 3514–3521. [CrossRef]
9. Ghosh, A.N.; Klimczak, M.; Buczynski, R.; Dudley, J.M.; Sylvestre, T. Supercontinuum generation in heavy-metal oxide glass based suspended-core photonic crystal fibers. *J. Opt. Soc. Am. B* **2018**, *35*, 2311–2316. [CrossRef]
10. Jamatia, P.; Saini, T.S.; Kumar, A.; Sinha, R.K. Design and analysis of a highly nonlinear composite photonic crystal fiber for supercontinuum generation: Visible to mid-infrared. *Appl. Opt.* **2016**, *55*, 6775–6781. [CrossRef]
11. Monfared, Y.E.; Ponomarenko, S.A. Slow light generation in liquid-filled photonic crystal fibers via stimulated Brillouin scattering. *Optik Int. J. Light Electron. Opt.* **2016**, *127*, 5800–5805. [CrossRef]
12. Monfared, Y.E.; Ponomarenko, S.A. Highly Nonlinear Liquid-filled Photonic Crystal Fibers. In Proceedings of the Photonics North 2015, Ottawa, ON, Canada, 9–11 June 2015.
13. Chaudhari, C.; Liao, M.; Suzuki, T.; Ohishi, Y. Chalcogenide Core Tellurite Cladding Composite Microstructured Fiber for Nonlinear Applications. *J. Lightw. Technol.* **2012**, *30*, 2069–2076. [CrossRef]
14. Liao, M.; Chaudhari, C.; Qin, G.; Yan, X.; Kito, C.; Suzuki, T.; Ohishi, Y.; Matsumoto, M.; Misumi, T. Fabrication and characterization of a chalcogenide-tellurite composite microstructure fiber with high nonlinearity. *Opt. Express* **2009**, *17*, 21608–21614. [CrossRef] [PubMed]
15. Han, T.; Liu, Y.; Wang, Z.; Guo, J.; Wu, Z.; Wang, S.; Li, Z.; Zhou, W. Unique characteristics of a selective-filling photonic crystal fiber Sagnac interferometer and its application as high sensitivity sensor. *Opt. Express* **2013**, *21*, 122–128. [CrossRef] [PubMed]
16. Monfared, Y.E.; Liang, C.; Khosravi, R.; Korocovska, B.; Yang, S. Selectively toluene-filled photonic crystal fiber Sagnac interferometer for temperature sensing applications. *Results Phys.* **2019**, *13*, 102297. [CrossRef]

17. Islam, M.S.; Sultana, J.; Dinovitser, A.; Faisal, M.; Islam, M.R.; Abbott, D. Zeonex-based asymmetrical terahertz photonic crystal fiber for multichannel communication and polarization maintaining applications. *Appl. Opt.* **2018**, *57*, 666–672. [CrossRef]
18. Zu, P.; Chan, C.C.; Siang, L.W.; Jin, Y.; Zhang, Y.; Fen, L.H.; Chen, L.; Dong, X. Magneto-optic fiber Sagnac modulator based on magnetic fluids. *Opt. Lett.* **2011**, *36*, 1425–1427. [CrossRef]
19. Cho, T.; Kim, G.; Lee, K.; Lee, S.; Jeong, J. Study on the Fabrication Process of Polarization Maintaining Photonic Crystal Fibers and Their Optical Properties. *J. Opt. Soc. Korea* 2008, *12*, 19–24. [CrossRef]
20. Monfared, Y.E.; Ahmadian, A. Broadband dispersion compensating using rectangular-lattice photonic crystal fiber. *Phys. Script* **2013**, *T157*, 014017. [CrossRef]
21. Zhu, Z.; Brown, T.G. Full-vectorial finite-difference analysis of microstructured optical fibers. *Opt. Express* **2002**, *10*, 853–864. [CrossRef]
22. Jiang, W.; Shen, L.; Chen, D.; Chi, H. An Extended FDTD Method With Inclusion of Material Dispersion for the Full-Vectorial Analysis of Photonic Crystal Fibers. *J. Lightw. Technol.* **2006**, *24*, 4417–4423. [CrossRef]
23. Monfared, Y.E.; Maleki, Javan, A.R.; Monajati Kashani, A.R. Confinement loss in hexagonal lattice photonic crystal fibers. *Optik Int. J. Light Electron. Opt.* 2013, *124*, 7049–7052. [CrossRef]
24. Lee, Y.S.; Lee, C.G.; Jung, Y.; Kim, S. Diamond unit cell photonic crystal fiber with high birefringence and low confinement loss based on circular air holes. *Appl. Opt.* 2015, *54*, 6140–6145. [CrossRef] [PubMed]
25. Brill, L.; Troles, J.; Houziot, P.; Desevedavy, F.; Coulombier, Q.; Renversez, G.; Chartier, T.; Nguyen, T.N.; Adam, J.; Tryanor, N. Interfaces impact on the transmission of chalcogenides photonic crystal fibres. *J. Ceram. Soc. Jpn.* **2008**, *116*, 1024–1027. [CrossRef]
26. Lee, Y.S.; Lee, C.G.; Jung, Y.; Oh, M.; Kim, S. Highly Birefringent and Dispersion Compensating Photonic Crystal Fiber Based on Double Line Defect Core. *J. Opt. Soc. Korea* **2016**, *20*, 567–574. [CrossRef]
27. Sharma, M.; Borogohain, N.; Konar, S. Index Guiding Photonic Crystal Fibers With Large Birefringence and Walk-Off. *J. Lightw. Technol.* **2013**, *31*, 3339–3344. [CrossRef]